PENSOFT

SENCKENBERG
NATURE RESEARCH

Leibniz Association

Phylogenetic relationships among four superfamilies in Tanaidacea (Peracarida) inferred from mitochondrial genomes

Yoshinobu Matsushima[1], Yasunori Kano[2], Keiichi Kakui[3]

1 *Department of Natural History Sciences, Graduate School of Science, Hokkaido University, Sapporo 060-0810, Japan*

2 *Atmosphere and Ocean Research Institute, The University of Tokyo, Kashiwa 277-8564, Japan*

3 *Department of Biological Sciences, Faculty of Science, Hokkaido University, Sapporo 060-0810, Japan*

Corresponding author: Yoshinobu Matsushima (mattuu901@eis.hokudai.ac.jp)

Received 21 March 2026
Accepted 09 July 2026
Published 19 August 2026

Academic Editors Martin Schwentner, Klaus-Dieter Klass

Citation: Matsushima Y, Kano Y, Kakui K (2026) Phylogenetic relationships among four superfamilies in Tanaidacea (Peracarida) inferred from mitochondrial genomes. Arthropod Systematics & Phylogeny 84: 705–718. https://doi.org/10.3897/asp.84.e192470

Abstract

Tanaidacea contains about 1600 species across four superfamilies (Apseudoidea, Neotanaoidea, Paratanaoidea, and Tanaidoidea). Phylogenetic relationships among the four superfamilies had been investigated molecularly with one to several genes, or with transcriptome data, but not with mitochondrial genome (mitogenome) data. Mitogenome data were available only for *Pseudotanais* sp. (Paratanaoidea) and *Arctotanais alascensis* (Tanaidoidea). We sequenced and annotated a complete mitogenome sequence for *Sinelobus kisui* (Tanaidoidea) and nearly complete mitogenome sequences for *Apseudes nipponicus*, *Apseudes ranma*, *Carpoapseudes spinigena* (Apseudoidea), and *Neotanais* sp. (Neotanaoidea). We detected the typical two rRNA and 13 protein-coding genes (PCGs) in all five species, but failed to detect one to five tRNAs in each species. The gene orders of the four superfamilies differed from the pancrustacean ground pattern and from one another. In maximum-likelihood phylogenetic trees based on amino acid and nucleotide datasets for the 13 PCGs and two rRNA genes, Tanaidacea emerged as a weakly supported sister clade to Isopoda. Within Tanaidacea, a fully supported Apseudoidea was the sister group to a moderately supported clade comprising the other three superfamilies; in the latter clade, a weakly supported Tanaidoidea clade was successively sister to Paratanaoidea and then to Neotanaoidea. The mitogenome-based topology among the four superfamilies differed from previous topologies based on 18S rRNA or transcriptome data (Apseudoidea, (Paratanaoidea, (Neotanaoidea, Tanaidoidea))). This contradiction suggests possible effects of mito–nuclear discordance or long-branch attraction for *Pseudotanais* sp. and *S. kisui*.

Keywords

Apseudoidea, mitochondrion, Neotanaoidea, Paratanaoidea, Tanaidoidea

1. Introduction

Tanaidacea, one of the 12 extant orders in the crustacean superorder Peracarida, comprises about 1600 species (WoRMS 2026). Most species are marine and benthic and are only a few millimeters long. Most recent molecular phylogenetic studies (e.g., Schwentner et al. 2018; Bernot et al. 2023; Yu et al. 2024; Jakiel et al. 2025;

Barta et al. 2025) supported close relationships among Tanaidacea, Isopoda, and Cumacea, which form a "Mancoida" clade. The currently accepted classification of extant Tanaidacea is a two-suborder, four-superfamily system: suborder Apseudomorpha comprising superfamily Apseudoidea (15 families), and suborder Tanaidomorpha comprising the superfamilies Neotanaoidea (one family), Paratanaoidea (24 families), and Tanaidoidea (one family) (WoRMS 2026).

Phylogenetic relationships among the superfamilies in Tanaidacea have received limited molecular investigation. Kakui et al. (2011), which included representative taxa from all four superfamilies for the first time and was based on 18S rRNA gene sequences from 31 tanaidacean and two isopod species (outgroup), found that (1) Neotanaoidea and Tanaidoidea formed a clade, which was the sister group to Paratanaoidea, collectively forming Tanaidomorpha; and (2) Apseudoidea (= Apseudomorpha) was recovered as a weakly supported monophyletic group or was paraphyletic to Tanaidomorpha. Araújo-Silva (2016) reconstructed a phylogeny based on a supermatrix dataset that consists of the cytochrome *c* oxidase subunit I (COI), Histone H3, and 28S rRNA genes from 24 tanaidacean and three isopod species, and found both suborders to be monophyletic. Relationships among the three tanaidomorph superfamilies were identical to those in Kakui et al. (2011). Kakui et al. (2021) reconstructed a phylogeny based on 22 tanaidacean and one isopod transcriptomes (the final alignment comprising 9462 amino acids). This analysis fully supported monophyly for the two suborders and four superfamilies, and again confirmed the relationships among the three tanaidomorph superfamilies in Kakui et al. (2011). Although the higher-level relationships within Tanaidacea seemed to have thus been sufficiently resolved, many families were not included in previous molecular datasets, and additional molecular markers remain to be explored.

Mitochondrial genome (or mitogenome) data have not yet been used to investigate phylogenetic relationships among the four superfamilies in Tanaidacea. Although mitogenomes generally contain less phylogenetic information than transcriptomes, they still provide substantially more information than one or a few gene markers. In addition, mitogenomes can be sequenced from specimens preserved for taxonomic purposes (e.g., ethanol or formalin fixation), making them more available for data acquisition than transcriptomes, which require samples to be freshly collected, deep-frozen, or fixed in RNA-stabilization reagents.

At the onset of this study, mitogenome sequences were available for the tanaidoid *Arctotanais alascensis* (Kakui and Kano 2021) and the paratanaoid *Pseudotanais* spp. (Jakiel et al. 2025), but none from apseudoids or neotanaoids. We sequenced and annotated the complete or nearly complete mitogenomes for five tanaidaceans, including the first mitogenomes from apseudoid and neotanaoid taxa. We then analyzed the mitochondrial gene order of all seven available tanaidacean mitogenomes and reconstructed a phylogenomic tree to infer the relationships among the four superfamilies.

2. Materials and methods

2.1. Sampling, DNA extraction, seed sequence determination, and long PCR

We used individual specimens identified as the following five species collected around Japan: (1) *Apseudes nipponicus* Shiino, 1937 (Apseudoidea: Apseudidae), collected from an open-air experimental aquarium in the Shimoda Marine Research Center (University of Tsukuba), Shizuoka, Japan (for details, see Kakui et al. 2017). (2) *Apseudes ranma* Matsushima and Kakui, 2024, collected from an aquarium tank in the Port of Nagoya Public Aquarium, Aichi, Japan (for details, see Kakui and Hiruta 2013); this specimen was a descendant of a single hermaphrodite isolated in March 2019 (for details, see Matsushima and Kakui 2024). (3) *Carpoapseudes spinigena* Bamber, 2007 (Apseudoidea: Apseudidae), collected at 1028–1075 m depth off the southeastern coast of Hokkaido, Japan (for details, see Kakui et al. 2020). (4) *Neotanais* sp. (Neotanaoidea: Neotanaidae), collected at 1018–1042 m depth, East China Sea (29.322500°N, 127.622900°E to 29.341983°N, 127.632633°E), Japan, on 21 November 2009 during Cruise N295 of TRV Nagasaki-maru (Nagasaki University). (5) *Sinelobus kisui* Hirano and Kakui, 2022 (Tanaidoidea: Tanaididae), collected from a brackish stream at Hagi, Yamaguchi, Japan (for details, see Hirano and Kakui 2022). All specimens were fixed in 80–99% ethanol and preserved in 99% ethanol.

Total DNA was extracted from the whole body of each individual by using a NucleoSpin Tissue XS Kit (Macherey–Nagel, Germany). As seed sequences, previously determined partial COI sequences were used for *A. ranma* (LC791470; Matsushima and Kakui 2024) and *C. spinigena* (LC545558; Kakui et al. 2020), and newly determined sequences for *A. nipponicus*, *Neotanais* sp., and *S. kisui*. Primers LCO1490 and HCO2198 (Folmer et al. 1994) were used for PCR and cycle sequencing. PCR amplification conditions for COI with TaKaRa Ex Taq DNA polymerase (TaKaRa Bio, Japan) were 94°C for 1 min; 35 cycles of 98°C for 10 s, 42–50°C for 30 s, and 72°C for 1 min; and 72°C for 2 min. Nucleotide sequences were determined with a BigDye Terminator Kit v3.1 and a 3730 DNA Analyzer (Life Technologies, USA).

For *S. kisui*, we designed primer pair Sk_COI_LF (5'-TCCTATAGGTGGGGGTGATCCAATTTTATTTCAGC-3') and Sk_COI_LR (5'-CTATATGCAGCCAAGGATAGCGGTGGGTAAATTG-3'), by using Primer3Plus (Untergasser et al. 2007) and based on the determined COI sequence, to amplify the nearly complete mitogenome by long PCR. The long-PCR amplification conditions with KOD ONE PCR Master Mix (Toyobo, Japan) were 45 cycles of 98°C for 10 s, 68°C for 5 s, and 68°C for 3 min. Amplicons were purified with the Extractor PCR & Gel Clean Up Kit (Toyobo).

We used the purified amplicon of *S. kisui* and DNA extracted from each of the other four species in the whole-genome shotgun sequencing described below.

2.2. Mitogenome sequencing and assembly

Whole-genome shotgun sequencing was performed by using 2 × 200 bp (*A. nipponicus*) and 2 × 150 bp (*A. ranma*, *C. spinigena*, and *Neotanais* sp.) paired-end reads on the DNBSEQ-G400 platform (MGI Tech, China) at Bioengineering Lab Co., Japan. Sequencing for *S. kisui* was performed by using 2 × 150 bp paired-end reads on the DNBSEQ-G400RS platform at Genome Read Inc., Japan. A total of 32,444,610 reads (2 × 4.8 Gbp) were obtained for *A. nipponicus*; 17,433,684 (2 × 3.4 Gbp) for *A. ranma*; 32,127,279 (2 × 4.7 Gbp) for *C. spinigena*; 34,957,034 (2 × 5.2 Gbp) for *Neotanais* sp.; and 6,228,917 (2 × 1.87 Gbp) for *S. kisui*.

The quality of the raw FASTQ files was initially assessed by using FastQC v0.12.0 (Andrews 2010) with default parameters. Adapter sequences were subsequently trimmed from the raw reads by using fastp v1.0.1 (Chen et al. 2018). All processed reads were assembled into target genomes by using GetOrganelle v1.7.7.1 (Jin et al. 2020) on the Galaxy web platform (The Galaxy Community 2024), with a COI sequence acting as a seed for the assembly process. For *S. kisui*, the contig obtained and the partial COI sequence were concatenated in MEGA11 (Tamura et al. 2021). To verify the assembled genomes, the paired-end reads were mapped back to their respective assembled genomes using BWA-MEM v0.7.19 (Li 2013). The reads aligning to target genes were extracted into FASTQ format with SAMtools v1.9 (Danecek et al. 2021), and the final mapped reads were visualized and interpreted by using Integrative Genomics Viewer (IGV) v2.19.5 (Thorvaldsdóttir et al. 2013).

Based on the assembled genomes of *A. nipponicus*, *A. ranma*, and *Neotanais* sp., we designed the following primers by using Primer3Plus and OlvTools (https://olvtools.com/tmvalue) to determine the sequences that remained unassembled after the procedure described above: ApnF (5'-GTATCCCTTTCCCGCCCTGCATCAC-3') and ApnR (5'-CACACATTTCGTGCTCCCCTTTGATC-3') for *A. nipponicus*; AprF (5'-CAGGATACACTTTTCGTGCTCCTCTTTG-3') and AprR (5'-CCCCAGCCTCAGGTTTTAAATGAAG-3') for *A. ranma*; and NeoF (5'-GTCGTGTTTTAGTTGCTTGGTCTGCACTTC-3') and NeoR (5'-CCACGCAACACTATAACTGCCCAAATCATC-3') for *Neotanais* sp. PCR amplification conditions with KOD ONE PCR Master Mix were as follows: for *A. nipponicus*, 45 cycles of 98°C for 10 s, 60°C for 5 s, and 68°C for 30 s; for *A. ranma*, 45 cycles of 98°C for 10 s, 55°C for 5 s, and 68°C for 30 s; and for *Neotanais* sp., 45 cycles of 98°C for 10 s and 68°C for 5 s. The amplified sequences were determined with a BigDye Terminator Kit v3.1 and a 3730 DNA Analyzer.

2.3. Mitogenome annotation

In addition to annotating the sequences of the five species determined in this study, we re-annotated the previously published mitogenome of *Arctotanais alascensis* (LC597489; Kakui and Kano 2021), which had been annotated by using the MITOS webserver (Bernt et al. 2013). Initial annotation was performed with MITOS2 (Donath et al. 2019) on the Galaxy web platform (The Galaxy Community 2024). Protein-coding genes (PCGs) not identified by MITOS2 were searched with the Open Reading Frame Finder (ORF Finder) provided by the National Center for Biotechnology Information (https://www.ncbi.nlm.nih.gov/orffinder). All the PCG candidate regions were translated by using the invertebrate mitochondrial genetic code, and their gene identities were confirmed with reciprocal BLASTP (Altschul et al. 1990) and by searching against the Conserved Domain Database (Lu et al. 2020). Based on these alignments, start and stop codons were identified manually.

Genes that remained unidentified were identified manually through comparative alignments. The atp8 gene in *A. ranma* was determined by aligning the assembled genome with that of *A. nipponicus*, using MUSCLE (Edgar 2004) in MEGA11. After identifying putative rrnL sequences (1092 bp for *A. nipponicus* and 598 bp for *A. ranma*) by using Barrnap v0.9 (Seemann 2018), the definitive sequences were determined by aligning them with the rrnL of *C. spinigena*, using MUSCLE. Additional tRNA searches were conducted by using ARWEN v1.2.3 (Laslett and Canbäck 2008) and tRNAscan-SE v2.0 (Chan et al. 2021). ARWEN successfully detected trnD and trnI in *A. alascensis* and trnR in *Neotanais* sp., none of which had been identified by MITOS2. Manual curation and editing of the mitogenomes were performed by using UGENE v52.1 (Okonechnikov et al. 2012).

The annotated mitochondrial genome sequences determined in this study have been deposited in the DDBJ/EMBL/GenBank databases under accession numbers LC923624–LC923628.

2.4. Phylogenetic analyses

The concatenated dataset of 13 PCGs and two rRNAs included sequences from seven tanaidacean species, 71 non-tanaidacean peracarid species (41 amphipods, one cumacean, 25 isopods, one lophogastrid, two mysids, and one stygiomysid), and two non-peracarid species (one decapod and one euphausiacean) (Dataset 1; Table S1). Nucleotide sequences for the PCGs from all species except *Pseudotanais* sp. were translated into amino acid sequences according to the invertebrate mitochondrial genetic code. For *Pseudotanais* sp., translation with that code was not possible (the codon TAA translates as tyrosine rather than a stop codon; Jakiel et al. 2025). We thus used the amino acid sequences provided in the GenBank CDS features. The amino acid sequences were aligned by using the L-INS-i algorithm (Katoh et al. 2005) implemented in MAFFT v7.526 (Katoh and Standley 2013) and subsequently back-translated to nucleotide sequences by using PAL2NAL v14 (Suyama et al. 2006). For *Pseudotanais* sp., the back-translated aligned nucleotide sequences were replaced with the original sequences, retaining the gap positions in the back-translated sequences.

The rRNAs were aligned by using the Q-INS-i algorithm (Katoh and Toh 2008) in MAFFT v7.526. Poorly aligned regions were removed by using trimAl (Capella-Gutiérrez et al. 2009). After the final alignment, Dataset 1 was 11,650 positions long. The optimal substitution model for 41 partitions (three codon positions for the 13 PCGs + two rRNAs) for Dataset 1 was determined by using ModelFinder (Kalyaanamoorthy et al. 2017) with the MFP+MERGE option, based on the Bayesian information criterion (BIC), resulting in the consolidation of these 41 partitions into 22 partitions (File S1). A maximum likelihood (ML) analysis was performed by using IQ-TREE v3.0.1 (Wong et al. 2026) under the bnni option (Hoang et al. 2018). Branch support values were obtained from an ultrafast bootstrap analysis of 10,000 pseudoreplicates (UFBoot; Hoang et al. 2018). Branches with UFBoot ≥ 95% were regarded as strongly supported. The resulting phylogenetic tree was visualized by using FigTree v1.4.4 (Rambaut 2018) (File S1).

The initial analysis with IQ-TREE detected extensive substitutional saturation in Dataset 1, particularly at third-codon positions in the PCGs. We thus do not present the results from Dataset 1, but instead analyzed two new datasets derived from Dataset 1. Dataset 2 included amino-acid sequences for the 13 PCGs and nucleotide sequences for the two rRNAs; that is, the aligned amino acid sequences were not back-translated to nucleotide sequences. Dataset 3 included nucleotide sequences for the first and second codon positions of the 13 PCGs and for the two rRNAs; that is, the nucleotides in the third codon position were removed from Dataset 1.

Dataset 2 comprised 4518 positions. The initial 15 partitions were merged into 13 optimal partitions by using ModelFinder with the MFP+MERGE option based on the BIC. Table S2 presents the final partitions and optimized substitution models. Dataset 3 comprised 8182 positions. The initial 28 partitions were merged into 17 optimal partitions by using ModelFinder with the MFP+MERGE option based on the BIC. Table S3 presents the final partitions and optimized substitution models. Methods for the ML analyses, branch support estimation, and drawing of the trees were as described above for Dataset 1.

To assess whether long-branch attraction (LBA) artifacts (Bergsten 2005) affected the relationships within Tanaidomorpha, we performed parametric simulations using AliSim (Ly-Trong et al. 2022) in IQ-TREE. We simulated 100 artificial alignments under the assumption that the true evolutionary process was represented by the partitioning scheme, optimized substitution models, and parameter estimates obtained from Dataset 2 (comprising amino acid sequences of the 13 PCGs and nucleotide sequences of the two rRNAs). The simulations were performed using an ML tree constrained to recover Tanaidoidea and Neotanaoidea as sister groups. For each simulated dataset, we reconstructed an ML tree using IQ-TREE, applying these exact empirical settings of Dataset 2. Finally, the 100 resulting simulated ML trees were mapped onto the unconstrained ML tree to calculate the parametric bootstrap support values (PB) for each branch.

All sequence alignments used in this study have been deposited in the Figshare repository (Kakui 2026).

3. Results

3.1. Mitogenome assembly

The assembled genomes for *Apseudes nipponicus* and *Apseudes ranma* were single contigs, 14,717 bp and 14,599 bp long, respectively (Fig. 1A, B), each containing an unassembled region. Ten contigs (197–15,857 bp) were obtained for *Carpoapseudes spinigena* (Fig. 2A), with the longest contig containing PCGs, rRNAs, and tRNAs (Fig. 2B). The assembled genome for *Neotanais* sp. was recovered as a single contig 14,746 bp long (Fig. 3A) containing an unassembled region. The complete circular mitochondrial genome of *Sinelobus kisui* was determined, which is 14,126 bp long (Fig. 3B).

For *A. nipponicus* and *A. ranma*, multiple bands were observed in electrophoresis of the PCR products amplified with specific primers, preventing identification of the target sequences. Cycle sequencing was thus not carried out for these bands. In *Neotanais* sp., a single band of approximately 900 bp was obtained. Sequencing of this product successfully determined only a ~600-bp portion, which completely overlapped with and was identical to the terminal region of the 14,746-bp contig mentioned above, including the primer region.

Nucleotide composition varied markedly among the species (Figs 1–3), with the following GC contents: 42.60% in *A. nipponicus*, 40.77% in *A. ranma*, 34.33% in *C. spinigena*, 43.30% in *Neotanais* sp., and 20.64% in *S. kisui*.

3.2. Annotation

In the five species, 13 PCGs and two rRNAs were identified. The complete set of 22 tRNAs was not identified, with the following being absent: trnI and trnM in both *A. nipponicus* (Fig. 1A) and *A. ranma* (Fig. 1B); trnI, trnM, trnN, trnS1, and trnV in *C. spinigena* (Fig. 2B); trnI in *Neotanais* sp. (Fig. 3A); and trnD in *S. kisui* (Fig. 3B).

Our re-annotation of the mitogenome of *Arctotanais alascensis* identified trnI, which was not identified in Kakui and Kano (2021). The rrnL gene was 455 bp longer than annotated in Kakui and Kano (2021), and the extended portion of the gene included the whole length of the putative control region suggested by Kakui and Kano (2021).

3.3. Gene order

Figure 4 shows the gene order for seven tanaidacean mitogenomes and the hypothetical ground pattern for Pancrustacea (Boore et al. 1998). Gene order was identical in the two species of *Apseudes*. The PCG order was the

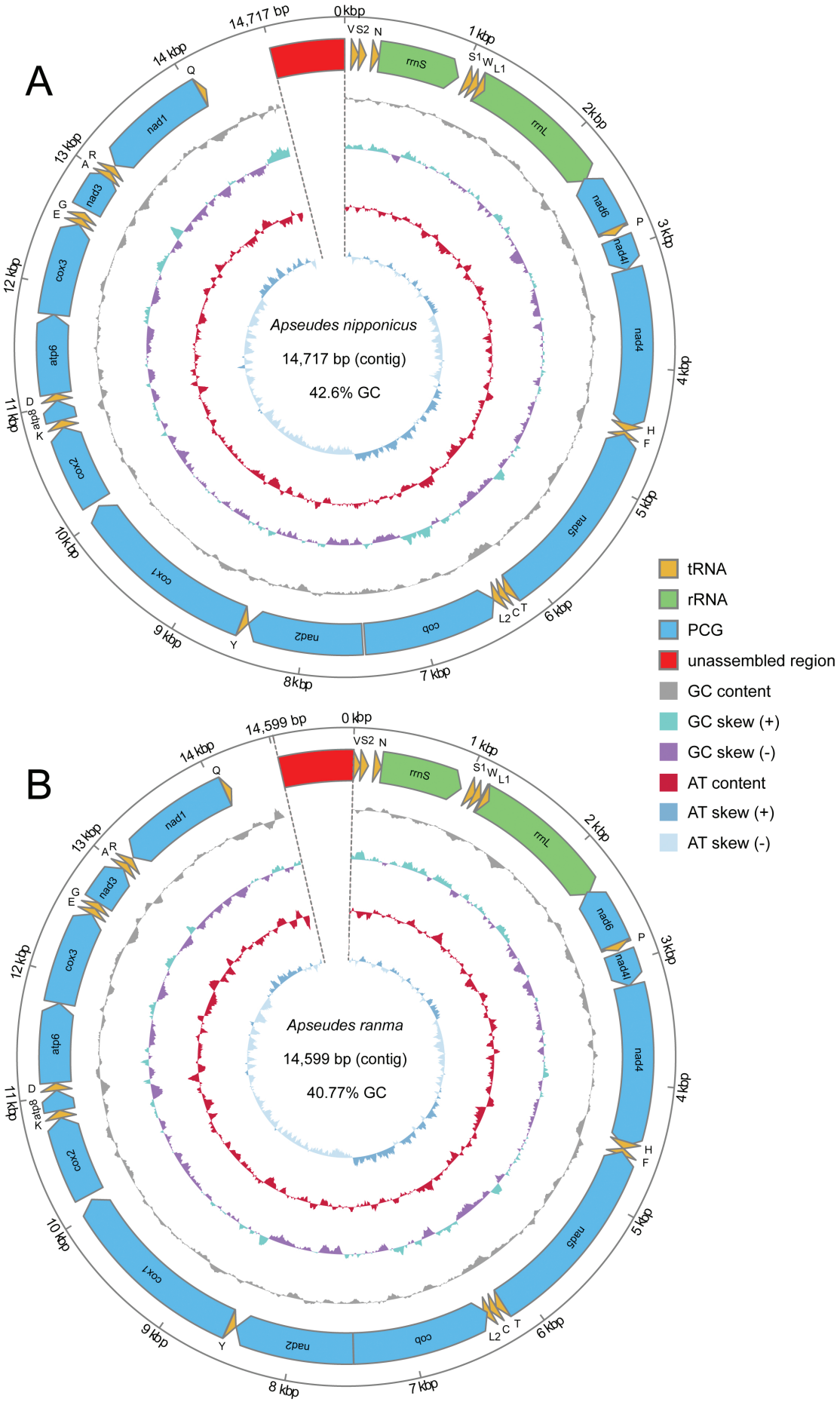

Figure 1. Maps of mitochondrial genomes visualized with gbdraw v0.7.0 (Kawato 2025, 2026). **A** *Apseudes nipponicus*. **B** *Apseudes ranma*. tRNA genes are labeled with their single-letter amino acid code; PCG, protein-coding gene.

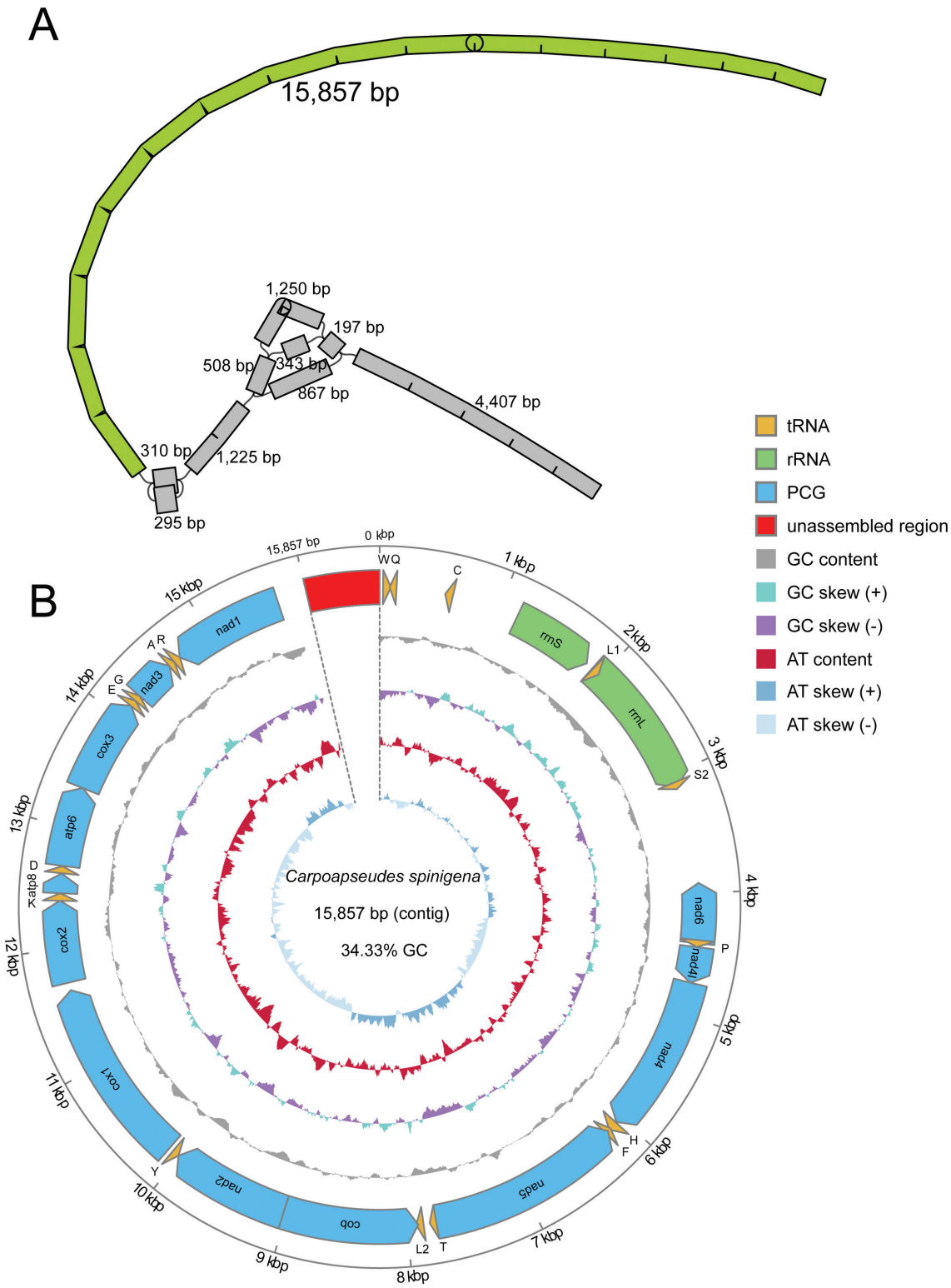

Figure 2. Assembly graph and gene map for *Carpoapseudes spinigena*. **A** All contigs visualized by using Bandage (Wick et al. 2015), with the longest contig highlighted in green. **B** Map of the mitochondrial genome derived from the longest contig, visualized by using gbdraw v0.7.0 (Kawato 2025, 2026). tRNA genes are labeled with their single-letter amino acid code; PCG, protein-coding gene.

same between *Carpoapseudes* and *Apseudes*, but there were several tRNA translocations. The three apseudoid mitogenomes shared three specific groupings, trnL1 + rrnL, nad6–trnT, and trnL2–nad1. No shared gene clusters were detected among the four tanaidomorph species examined, nor between the two tanaidoid species.

While all tanaidaceans studied exhibited gene arrangements distinct from the pancrustacean ground pattern, several ancestral clusters were observed (Fig. 4). These are [cox2 + trnK], [atp6 + cox3], [trnG + nad3 + trnA + trnR], [trnF + nad5], and [trnY + cox1] in the three apseudoids; [atp8 + atp6 + cox3 + trnG + nad3 + trnA], [nad4 +

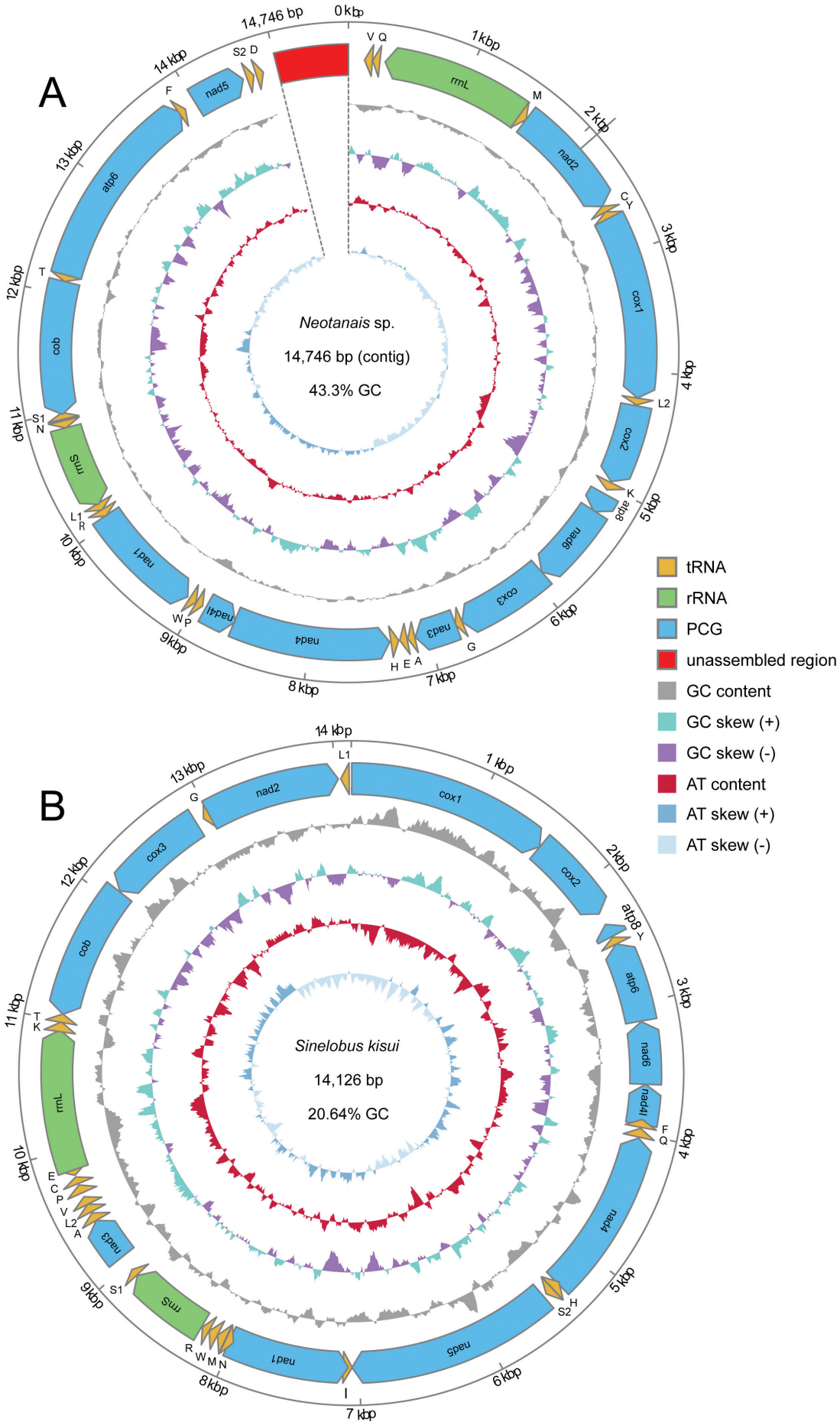

Figure 3. Mitochondrial genome maps visualized by using gbdraw v0.7.0 (Kawato 2025, 2026). **A** *Neotanais* sp. **B** *Sinelobus kisui*. tRNA genes are labeled with their single-letter amino acid code; PCG, protein-coding gene.

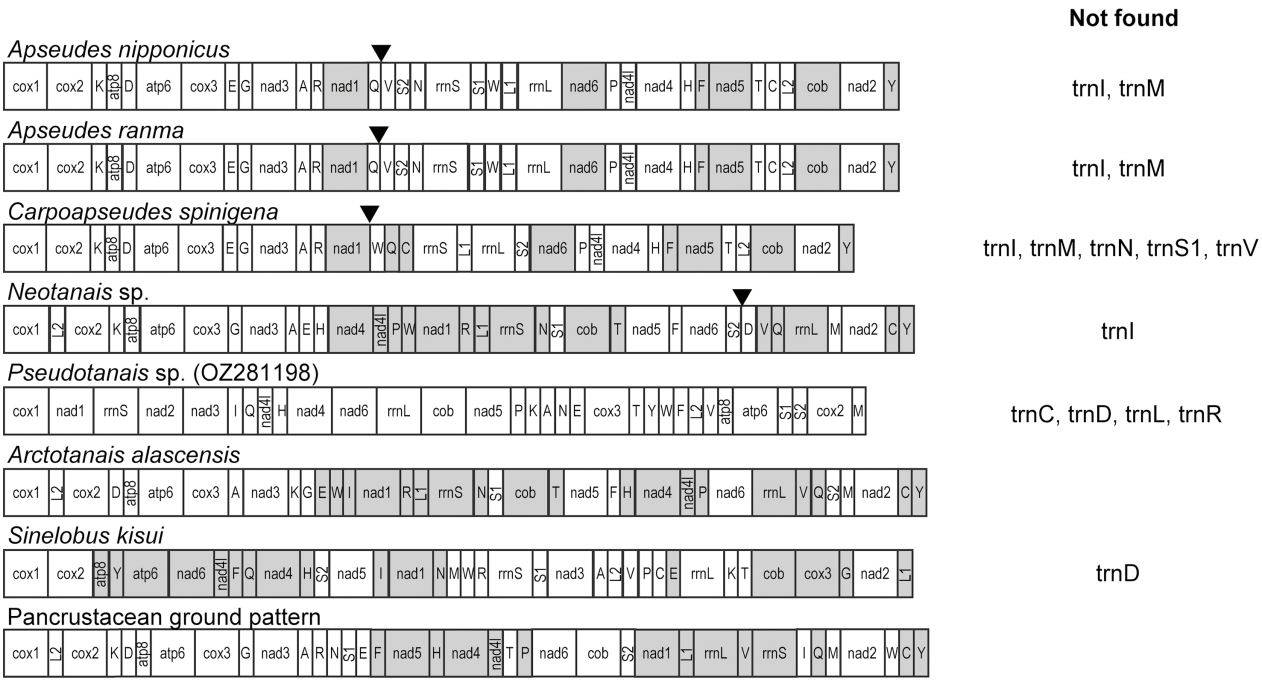

Figure 4. Comparison of gene order among tanaidaceans and the hypothetical ancestral pattern for Pancrustacea (Boore et al. 1998). Gray shading denotes genes on the reverse (–) strand. tRNA genes are labeled with their single-letter amino acid code. Arrowheads indicate the positions of unassembled regions.

nad4l], [trnM + nad2], and [trnC + trnY + cox1 + trnL2 + cox2 + trnK] in *Neotanais* sp.; [atp8 + atp6] in *Pseudotanais* sp.; and [nad3 + trnA] in the two tanaidoids.

3.4. Phylogeny

The ML trees based on Datasets 2 (Fig. 5) and 3 (Fig. 6) strongly support the monophyly of each of the peracarid orders that include two or more species in our analyses (UFBoot ≥ 98%). The interordinal relationships derived from the two datasets were identical except for the position of the "mysidacean" clade (= Mysida + Lophogastrida + Stygiomysida; cf. Meland et al. 2015). Branch support values also differed slightly between the two datasets. The mysidacean clade was sister to a strongly supported Mancoida clade (Cumacea + Isopoda + Tanaidacea) in Dataset 2 (Fig. 5) with weak support (UFBoot = 75%), but sister to the Amphipoda clade in Dataset 3 (Fig. 6) with even weaker support (UFBoot = 68%). The monophyly of Mancoida was supported with full or high support (UFBoot = 100% for Dataset 2; 98% for Dataset 3); the Isopoda + Tanaidacea clade was weakly supported in Dataset 2 (UFBoot = 64%) but moderately in Dataset 3 (UFBoot = 88%). In Dataset 1 (File S1), relationships among the orders were largely unresolved except for those among the three mysidacean orders; the monophyly of Tanaidacea received only weak support; and the mysidacean clade was recovered outside a weakly supported clade comprising the other peracarids.

The topology within Tanaidacea is identical between the two trees, with slight differences in branch support. The fully supported Apseudoidea clade was sister to the Tanaidomorpha clade (Tanaidoidea + Paratanaoidea + Neotanaoidea) with strong to moderate support (UFBoot = 99% for Dataset 2; 92% for Dataset 3). Within the latter clade, the neotanaoid *Neotanais* sp. lay outside a Paratanaoidea + Tanaidoidea clade, with weak (UFBoot = 76% for Dataset 2) or moderate (UFBoot = 92% for Dataset 3) support. The two tanaidoids formed a clade with high or low support (UFBoot = 97% for Dataset 2; 75% for Dataset 3). Our parametric simulations (Fig. S1) showed that a Paratanaoidea + Tanaidoidea clade was never reproduced in the simulated datasets (PB = 0%).

The branches leading to *Pseudotanais* sp. and *S. kisui* were markedly longer than those leading to the other five tanaidacean species (Figs 5, 6).

4. Discussion

4.1. Determined tanaidacean mitogenomes

We determined the complete, circular mitogenome for *S. kisui* and partial mitogenomes containing the complete set of PCGs and rRNAs and most tRNAs for the other four species. Our attempt to Sanger-sequence the unassembled regions in three species failed. Based on our observation in *Neotanais* sp. that the PCR amplicon sequence was identical to the terminal region of the long contig, the unassembled regions are suggested to be composed of long repeat sequences. To determine the complete mitogenomes of the species for which we were unable to obtain circular mitogenomes, long-read sequencing technologies may be necessary.

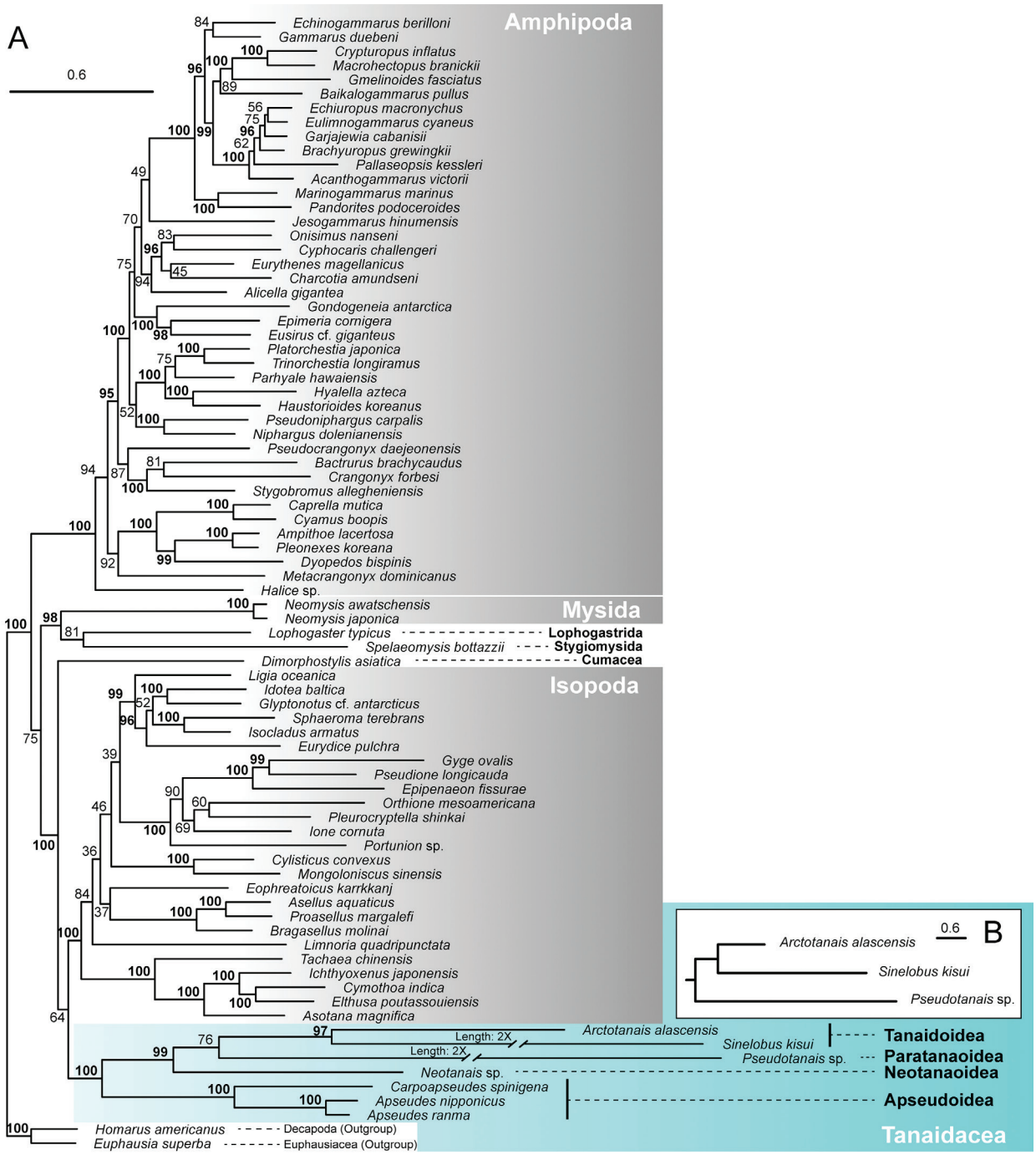

Figure 5. Maximum-likelihood (ML) phylogeny inferred from Dataset 2, including the amino acid sequences of the 13 PCGs and the nucleotide sequences of the two rRNAs (4518 characters; 13 partitions). **A** ML tree; double slashes indicate shortened branches. **B** Enlargement of part of the tree showing the true branch lengths leading to the three tanaidomorphs, *Arctotanais alascensis*, *Pseudotanais* sp., and *Sinelobus kisui*. Numbers near nodes are ultrafast bootstrap values (UFBoot). UFBoot ≥ 95%, indicating strong branch support, are in bold font. The scale bars indicate branch length in substitutions per site.

Our (re-)annotation showed that no typical control region (CR) was present in the circular mitogenomes of *A. alascensis* and *S. kisui*, and that the region previously annotated as the CR in *A. alascensis* corresponds to part of rrnL (Fig. 3B). The non-coding regions in these two species were less than 215 bp long. As suggested for some other crustaceans (Pons et al. 2014), their CR may be extremely short. We also failed to identify the CR in the partial mitogenomes of *A. nipponicus*, *A. ranma*, *C. spinigena*, and *Neotanais* sp. Their CRs may lie in the unassembled region. Although Jakiel et al. (2025) did not elaborate, the mitogenome of their *Pseudotanais* sp. has a long non-coding region that potentially contained a CR.

4.2. Gene order

We found that mitogenome gene order in Tanaidacea varies markedly among superfamilies and is highly divergent from the putative pancrustacean ground pattern. In

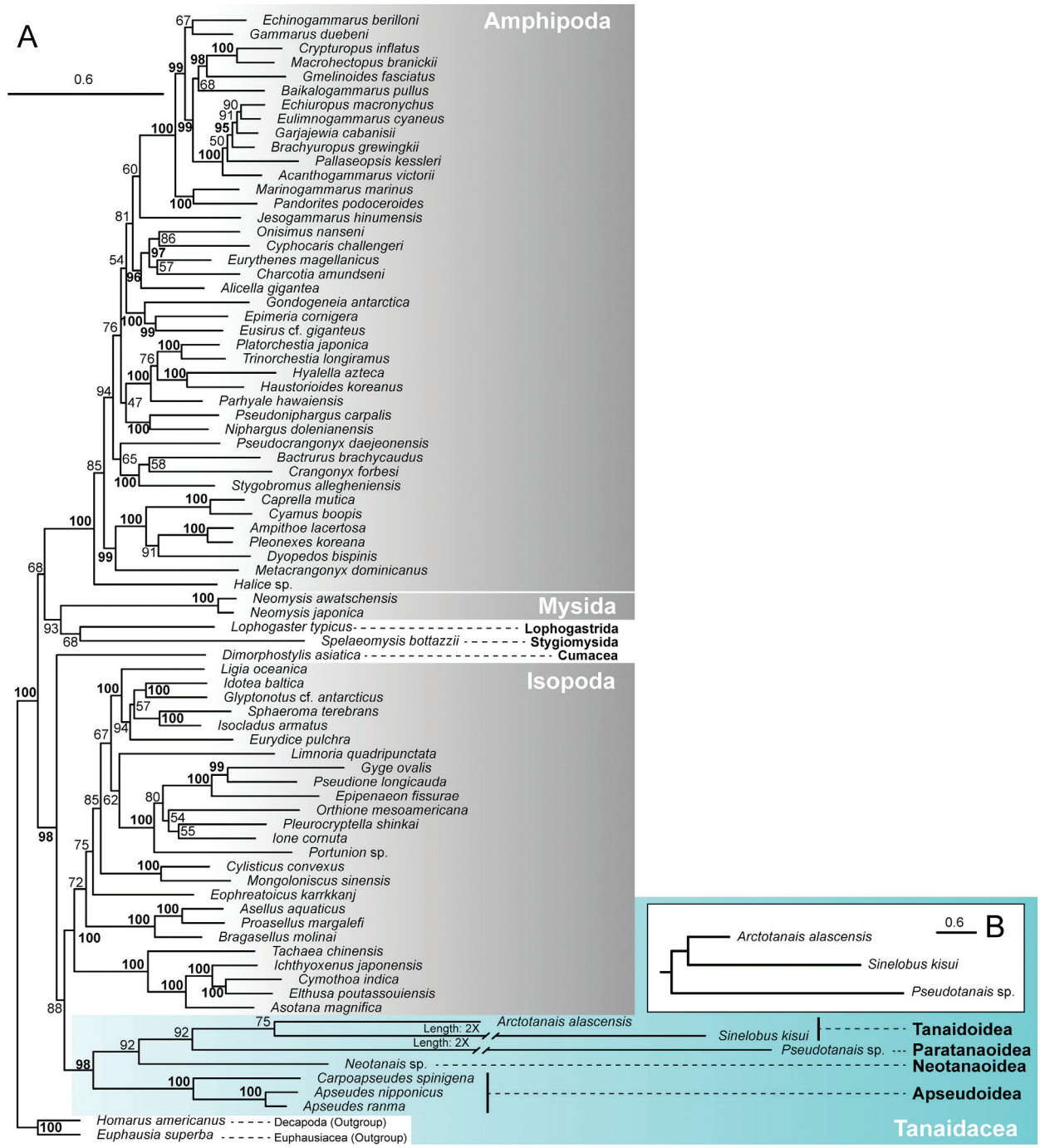

Figure 6. Maximum-likelihood (ML) phylogeny inferred from Dataset 3, including nucleotide sequences of the 13 PCGs (first and second codon positions only) and of the two rRNAs (8182 characters; 17 partitions). **A** ML tree; double slashes indicate shortened branches. **B** Enlargement of part of the tree showing the true branch lengths leading to the three tanaidomorphs, *Arctotanais alascensis*, *Pseudotanais* sp., and *Sinelobus kisui*. Numbers near nodes are ultrafast bootstrap values (UFBoot). UFBoot ≥ 95%, indicating strong branch support, are in bold font. The scale bars indicate branch length in substitutions per site.

addition, gene order stability varied considerably. Gene order was highly conserved in the two studied genera in Apseudoidea, whereas extensive rearrangements were evident in the two studied genera in Tanaidoidea.

Pseudotanais sp., *A. alascensis*, and *S. kisui* shared only one short cluster with the pancrustacean ground pattern, indicating a highly divergent mitogenome gene order. These three species, especially *Pseudotanais* sp. and *S. kisui*, exhibited much longer branch lengths than other tanaidaceans in our tree, which suggests that a marked acceleration in molecular evolutionary rates may have occurred in their most recent common ancestor. Previous studies have reported that higher substitution rates are correlated with elevated rates of gene rearrangements (Shao et al. 2003; Su et al. 2025), and this could account for the highly divergent gene order observed in these three species.

Höpel et al. (2022) reported that mitogenomes in representatives of three mysidacean orders (Lophogastrida, Stygiomysida, and Mysida) lack shared derived gene or-

ders and exhibit high levels of rearrangements. Similarly, in Tanaidacea, the fluidity of gene arrangement and changes in tRNA secondary structures are likely elevated. This high plasticity may have contributed to the difficulty of annotation and previous failures to detect trnI. While such extensive rearrangements are generally explained by the tandem duplication and random loss (TDRL) model, more complex rearrangements, such as those observed in *Pseudotanais* sp. and *S. kisui*, may stem from unknown transposition mechanisms involving recombination and double-stranded break repair (Luo et al. 2015).

4.3. Phylogeny

In the trees from Datasets 2 and 3, Tanaidacea was embedded in Mancoida as a strongly or fully supported clade, along with a cumacean species and a fully supported Isopoda clade. The sister taxon to Tanaidacea was not well resolved; an Isopoda + Tanaidacea clade appeared in both trees, but with only weak to moderate support. This sister relationship was recovered in a recent large-scale phylogenomic analysis (Iwasa-Arai et al. 2026), but not in other studies, which placed Tanaidacea as sister to Isopoda + Cumacea (Bernot et al. 2023; Barta et al. 2025).

The relationships we detected among tanaidacean superfamilies differ from those in three previous studies (Kakui et al. 2011, 2021; Araújo-Silva 2016). In our trees, Tanaidoidea is sister to Paratanaoidea, with only weak to moderate support, whereas the three previous studies recovered a Neotanaoidea + Tanaidoidea clade with high to full support. Our support values are insufficient to confidently overturn the robust topologies of previous studies, so this discrepancy requires careful interpretation. Our parametric simulations provide little evidence that the recovered Paratanaoidea + Tanaidoidea clade is an artifact of LBA. However, they cannot exclude the possibility that LBA arising from heterotachy – a phenomenon in which functional constraints on individual sites change over time, resulting in shifts in site-specific evolutionary rates (Lopez et al. 2002; Kolaczkowski and Thornton 2004) – contributed to the inferred relationship. Alternatively, the recovered relationship may reflect mito–nuclear discordance in the evolutionary history of Tanaidacea, a phenomenon reported in many other taxa, including algae (e.g., Kao et al. 2022), ants (e.g., Rahman et al. 2021), bears (e.g., Lammers et al. 2017), and fish (e.g., Baraf et al. 2025).

The long branches in *Pseudotanais* sp. and *S. kisui* might have been caused by a unique genetic code and a low-salinity habitat, respectively. In the mitogenome of *Pseudotanais* sp., TAA – normally a stop codon in the invertebrate mitochondrial genetic code – translates as tyrosine (Jakiel et al. 2025), which has not been observed in other peracarids. *Sinelobus kisui* is a brackish water species. Conrad et al. (2021) observed unique gene arrangements in fiddler crabs adapted to brackish environments, implying that habitat disparities exert specific selective pressures on the mitochondrial genome. Similar selective pressures may also have contributed to the long branch of *S. kisui* in the phylogenetic analysis.

This is the first phylomitogenomic analysis incorporating all of the four superfamilies in Tanaidacea. However, the taxonomic coverage is still highly limited: our dataset contains only seven of around 1600 known species; 14 apseudoid families and 23 paratanaoid families are not represented. It is unclear whether the high evolutionary rate observed in *Pseudotanais* sp., evident as a remarkably long branch, is common in Paratanaoidea. Aguinaldo et al. (1997) clarified the placement of Nematoda – previously difficult to resolve due to rapid evolution – by restricting their analysis to slowly evolving lineages. Likewise, adding more slowly evolving paratanaoid taxa may alter the inferred topology. Expanded mitogenome sequencing and phylogenetic analyses across a broader taxonomic range are needed to test whether the observed contradiction with nuclear genomic data represents genuine mito–nuclear discordance or LBA artifacts.

5. Declarations

Conflict of interest. The authors declare that they have no conflicts of interest in relation to this work.

Data Availability. The DNA sequence data underlying this study are available in the DDBJ/EMBL/GenBank databases under accession numbers LC923624–LC923628. All sequence alignments used in this study have been deposited in the Figshare repository (Kakui 2026). The other supporting data are available in the Supporting Information for this article (File S1; Tables S1–S3; Fig. S1).

6. Acknowledgements

We thank Jun Hashimoto for the opportunity to join TRV *Nagasaki-maru* cruise N295; Captain Hiroshi Yoshimura and the crew and researchers aboard the TRV *Nagasaki-maru* for help in collecting *Neotanais* sp.; Yasutaka Tsuchiya, Toshihiko Sato, Hideo Shinagawa, Yutaro Yamada, Daisuke Shibata, Atsuko Suzuki, Hiroaki Nakano, and Morihiko Tomatsuri for help in collecting *A. nipponicus*; Tsuyoshi Matsuda, Akira Ogushi, and Futoshi Kakizoe for help in collecting *A. ranma*; Hironori Komatsu for providing *C. spinigena*; Susumu Ohtsuka for help in collecting *S. kisui*; Hajime Ito for advice on long-PCR primer design; Samuel Abalde Lago for teaching analytical methods during the "Advanced Marine Biology Educational Program" at the Research Center for Marine Biology (RCMB), Tohoku University; Hiroaki Fukumori and the staff of RCMB for assistance; Satoshi Kawato, the developer of gbdraw Web App, for incorporating our requests; and Matthew H. Dick for reviewing the manuscript and editing our English. This study was funded in part by research grants from the Research Institute of Marine Invertebrates Foundation (KO2025-04, FY2025) and the Fujiwara Natural History Foundation (No. 17, FY2025); a JST SPRING grant JPMJSP2119; and KAKENHI grants JP19K06800, JP22H02681, JP23K23944, and JP26K09429 from the Japan Society for the Promotion of Science (JSPS).

7. References

Aguinaldo AMA, Turbeville JM, Linford LS, Rivera MC, Garey JR, Raff RA, Lake JA (1997) Evidence for a clade of nematodes, arthro-

pods and other moulting animals. Nature 387: 489–493. https://doi.org/10.1038/387489a0

Altschul SF, Gish W, Miller W, Myers EW, Lipman DJ (1990) Basic local alignment search tool. Journal of Molecular Biology 215: 403–410. https://doi.org/10.1016/s0022-2836(05)80360-2

Andrews S (2010) FastQC: A quality control tool for high throughput sequence data. Babraham Bioinformatics, Babraham Institute, Cambridge, United Kingdom. http://www.bioinformatics.babraham.ac.uk/projects/fastqc

Araújo-Silva CDL (2016) Taxonomy, systematics, morphological and molecular phylogeny of the order Tanaidacea (Crustacea: Peracarida), from the Antarctic, Atlantic and Pacific Oceans. Doctoral dissertation, Universidade do Porto (Portugal).

Baraf LM, Hung JY, Cowman PF (2025) Phylogenomics of marine angelfishes: Diagnosing sources of systematic discordance for an iconic reef fish family (F: Pomacanthidae). Systematic Biology 74: 799–817. https://doi.org/10.1093/sysbio/syaf016

Barta AC, Grams M, Bracken-Grissom H, Brix S, Cordeiro LM, Cummings B, Collins S, Farris WJ, Gerken S, Höpel CG, Lörz AN, McKim S, Meland K, Kruckenhauser L, Olesen J, Peres PA, Richter S, Wetzer R, Williams J, Kocot KM, Schwentner M (2025) Phylogenomics supports monophyly of marsupial crustaceans: a journey to direct development. bioRxiv. https://doi.org/10.1101/2025.11.06.686749

Bergsten J (2005) A review of long-branch attraction. Cladistics 21: 163–193. https://doi.org/10.1111/j.1096-0031.2005.00059.x

Bernot JP, Owen CL, Wolfe JM, Meland K, Olesen J, Crandall KA (2023) Major revisions in pancrustacean phylogeny and evidence of sensitivity to taxon sampling. Molecular Biology and Evolution 40: msad175. https://doi.org/10.1093/molbev/msad175

Bernt M, Donath A, Jühling F, Externbrink F, Florentz C, Fritzsch G, Pütz J, Middendorf M, Stadler PF (2013) MITOS: Improved de novo metazoan mitochondrial genome annotation. Molecular Phylogenetics and Evolution 69: 313–319. https://doi.org/10.1016/j.ympev.2012.08.023

Boore JL, Lavrov DV, Brown WM (1998) Gene translocation links insects and crustaceans. Nature 392: 667–668. https://doi.org/10.1038/33577

Capella-Gutiérrez S, Silla-Martínez JM, Gabaldón T (2009) trimAl: A tool for automated alignment trimming in large-scale phylogenetic analyses. Bioinformatics 25: 1972–1973. https://doi.org/10.1093/bioinformatics/btp348

Chan PP, Lin BY, Mak AJ, Lowe TM (2021) tRNAscan-SE 2.0: Improved detection and functional classification of transfer RNA genes. Nucleic Acids Research 49: 9077–9096. https://doi.org/10.1093/nar/gkab688

Chen S, Zhou Y, Chen Y, Gu J (2018) fastp: An ultra-fast all-in-one FASTQ preprocessor. Bioinformatics 34: i884–i890. https://doi.org/10.1093/bioinformatics/bty560

Conrad I, Craft A, Thurman CL, Baeza JA (2021) The complete mitochondrial genome of the red-jointed brackish-water fiddler crab *Minuca minax* (LeConte 1855) (Brachyura: Ocypodidae): New family gene order, and purifying selection and phylogenetic informativeness of protein coding genes. Genomics 113: 565–572. https://doi.org/10.1016/j.ygeno.2020.09.050

Danecek P, Bonfield JK, Liddle J, Marshall J, Ohan V, Pollard MO, Whitwham A, Keane T, McCarthy SA, Davies RM, Li H (2021) Twelve years of SAMtools and BCFtools. GigaScience 10: giab008. https://doi.org/10.1093/gigascience/giab008

Donath A, Jühling F, Al-Arab M, Bernhart SH, Reinhardt F, Stadler PF, Middendorf M, Bernt M (2019) Improved annotation of protein-coding genes boundaries in metazoan mitochondrial genomes. Nucleic Acids Research 47: 10543–10552. https://doi.org/10.1093/nar/gkz833

Edgar RC (2004) MUSCLE: Multiple sequence alignment with high accuracy and high throughput. Nucleic Acids Research 32: 1792–1797. https://doi.org/10.1093/nar/gkh340

Folmer O, Black M, Hoeh W, Lutz R, Vrijenhoek R (1994) DNA primers for amplification of mitochondrial cytochrome *c* oxidase subunit I from diverse metazoan invertebrates. Molecular Marine Biology and Biotechnology 3: 294–299.

Hirano K, Kakui K (2022) A new brackish tanaidacean, *Sinelobus kisui* sp. nov. (Crustacea, Peracarida, Tanaidacea), from Japan, with a key to *Sinelobus* species and barcode information from two loci. Zoosystematics and Evolution 98: 245–256. https://doi.org/10.3897/zse.98.84818

Hoang DT, Chernomor O, von Haeseler A, Minh BQ, Vinh LS (2018) UFBoot2: Improving the ultrafast bootstrap approximation. Molecular Biology and Evolution 35: 518–522. https://doi.org/10.1093/molbev/msx281

Höpel CG, Yeo D, Grams M, Meier R, Richter S (2022) Mitogenomics supports the monophyly of Mysidacea and Peracarida (Malacostraca). Zoologica Scripta 51: 603–613. https://doi.org/10.1111/zsc.12554

Iwasa-Arai T, Linse K, Andrade SC, Giribet G (2026) Unpouching Peracarida relationships with ultraconserved elements. Molecular Phylogenetics and Evolution 216: 108523. https://doi.org/10.1016/j.ympev.2025.108523

Jakiel M, Lubośny M, Błażewicz M, Burzyński A (2025) Decoding the evolutionary history and systematic complexity of Pseudotanaidae (Crustacea: Tanaidacea). Progress in Oceanography 238: 103534. https://doi.org/10.1016/j.pocean.2025.103534

Jin JJ, Yu WB, Yang JB, Song Y, dePamphilis CW, Yi TS, Li DZ (2020) GetOrganelle: A fast and versatile toolkit for accurate de novo assembly of organelle genomes. Genome Biology 21: 241. https://doi.org/10.1186/s13059-020-02154-5

Kakui K (2026) Sequence alignments for mitogenomic phylogenetic analyses in Matsushima et al. Figshare. https://doi.org/10.6084/m9.figshare.31530154

Kakui K, Fleming JF, Mori M, Fujiwara Y, Arakawa K (2021) Comprehensive transcriptome sequencing of Tanaidacea with proteomic evidences for their silk. Genome Biology and Evolution 13: evab281. https://doi.org/10.1093/gbe/evab281

Kakui K, Hiruta C (2013) Selfing in a malacostracan crustacean: why a tanaidacean but not decapods. Naturwissenschaften 100: 891–894. https://doi.org/10.1007/s00114-013-1079-5

Kakui K, Kano Y (2021) First complete mitochondrial genome of a tanaidacean crustacean (*Arctotanais alascensis*). Zoological Science 38: 267–272. https://doi.org/10.2108/zs200167

Kakui K, Katoh T, Hiruta SF, Kobayashi N, Kajihara H (2011) Molecular systematics of Tanaidacea (Crustacea: Peracarida) based on 18S sequence data, with an amendment of suborder/superfamily-level classification. Zoological Science 28: 749–757. https://doi.org/10.2108/zsj.28.749

Kakui K, Nomaki H, Komatsu H, Fujiwara Y (2020) Unexpected low genetic differentiation between Japan and Bering Sea populations of a deep-sea benthic crustacean lacking a planktonic larval stage (Peracarida: Tanaidacea). Biological Journal of the Linnean Society 131: 566–574. https://doi.org/10.1093/biolinnean/blaa106

Kakui K, Suzuki A, Nakano H, Kohtsuka H (2017) Habitat of a tanaidacean *Apseudes nipponicus* Shiino, 1937. Bulletin of the Ki-

takyushu Museum of Natural History and Human History, Series A (Natural History) 15: 1–3. https://doi.org/10.34522/kmnh.15.0_1

Kalyaanamoorthy S, Minh BQ, Wong TKF, von Haeseler A, Jermiin LS (2017) ModelFinder: Fast model selection for accurate phylogenetic estimates. Nature Methods 14: 587–589. https://doi.org/10.1038/nmeth.4285

Kao TT, Wang TH, Ku C (2022) Rampant nuclear–mitochondrial–plastid phylogenomic discordance in globally distributed calcifying microalgae. New Phytologist 235: 1394–1408. https://doi.org/10.1111/nph.18219

Katoh K, Kuma KI, Toh H, Miyata T (2005) MAFFT version 5: Improvement in accuracy of multiple sequence alignment. Nucleic Acids Research 33: 511–518. https://doi.org/10.1093/nar/gki198

Katoh K, Standley DM (2013) MAFFT multiple sequence alignment software version 7: Improvements in performance and usability. Molecular Biology and Evolution 30: 772–780. https://doi.org/10.1093/molbev/mst010

Katoh K, Toh H (2008) Recent developments in the MAFFT multiple sequence alignment program. Briefings in Bioinformatics 9: 286–298. https://doi.org/10.1093/bib/bbn013

Kawato S (2025) satoshikawato/gbdraw. GitHub. https://github.com/satoshikawato/gbdraw

Kawato S (2026) gbdraw: A genome diagram generator for microbes and organelles. bioRxiv. https://doi.org/10.64898/2026.04.07.716863

Kolaczkowski B, Thornton JW (2004) Performance of maximum parsimony and likelihood phylogenetics when evolution is heterogeneous. Nature 431: 980–984. https://doi.org/10.1038/nature02917

Lammers F, Janke A, Rücklé C, Zizka V, Nilsson MA (2017) Screening for the ancient polar bear mitochondrial genome reveals low integration of mitochondrial pseudogenes (Numts) in bears. Mitochondrial DNA Part B 2: 251–254. https://doi.org/10.1080/23802359.2017.1318688

Laslett D, Canbäck B (2008) ARWEN: A program to detect tRNA genes in metazoan mitochondrial nucleotide sequences. Bioinformatics 24: 172–175. https://doi.org/10.1093/bioinformatics/btm573

Li H (2013) Aligning sequence reads, clone sequences and assembly contigs with BWA-MEM. arXiv. https://doi.org/10.48550/arXiv.1303.3997

Lopez P, Casane D, Philippe H (2002) Heterotachy, an important process of protein evolution. Molecular Biology and Evolution 19: 1–7. https://doi.org/10.1093/oxfordjournals.molbev.a003973

Lu S, Wang J, Chitsaz F, Derbyshire MK, Geer RC, Gonzales NR, Gwadz M, Hurwitz DI, Marchler GH, Song JS, Thanki N, Yamashita RA, Yang M, Zhang D, Zheng C, Lanczycki CJ, Marchler-Bauer A (2020) CDD/SPARCLE: The conserved domain database in 2020. Nucleic Acids Research 48: D265–D268. https://doi.org/10.1093/nar/gkz991

Luo YJ, Satoh N, Endo K (2015) Mitochondrial gene order variation in the brachiopod *Lingula anatina* and its implications for mitochondrial evolution in lophotrochozoans. Marine Genomics 24: 31–40. https://doi.org/10.1016/j.margen.2015.08.005

Ly-Trong N, Naser-Khdour S, Lanfear R, Minh BQ (2022) AliSim: A fast and versatile phylogenetic sequence simulator for the genomic era. Molecular Biology and Evolution 39: msac092. https://doi.org/10.1093/molbev/msac092

Matsushima Y, Kakui K (2024) *Apseudes ranma* sp. nov. (Tanaidacea: Apseudidae) found in a public aquarium, with notes on phylogeny and a presumptive stridulatory organ. Bulletin of Marine Science 100: 451–469. https://doi.org/10.5343/bms.2024.0030

Meland K, Mees J, Porter M, Wittmann KJ (2015) Taxonomic review of the orders Mysida and Stygiomysida (Crustacea, Peracarida). PLoS ONE 10: e0124656. https://doi.org/10.1371/journal.pone.0124656

Okonechnikov K, Golosova O, Fursov M, Ugene Team (2012) Unipro UGENE: A unified bioinformatics toolkit. Bioinformatics 28: 1166–1167. https://doi.org/10.1093/bioinformatics/bts091

Pons J, Bauzà-Ribot MM, Jaume D, Juan C (2014) Next-generation sequencing, phylogenetic signal and comparative mitogenomic analyses in Metacrangonyctidae (Amphipoda: Crustacea). BMC Genomics 15: 566. https://doi.org/10.1186/1471-2164-15-566

Rahman MM, Hosoishi S, Ogata K (2021) Haplotype diversity and distribution pattern of *Oecophylla smaragdina* (Fabricius) (Hymenoptera, Formicidae) in Bangladesh based on mitochondrial COI genes. Journal of Asia-Pacific Entomology 24: 96–104. https://doi.org/10.1016/j.aspen.2020.11.010

Rambaut A (2018) FigTree. https://tree.bio.ed.ac.uk/software/figtree/

Schwentner M, Richter S, Rogers DC, Giribet G (2018) Tetraconatan phylogeny with special focus on Malacostraca and Branchiopoda: Highlighting the strength of taxon-specific matrices in phylogenomics. Proceedings of the Royal Society B 285: 20181524. https://doi.org/10.1098/rspb.2018.1524

Seemann T (2018) tseemann/barrnap. GitHub. https://github.com/tseemann/barrnap

Shao R, Dowton M, Murrell A, Barker SC (2003) Rates of gene rearrangement and nucleotide substitution are correlated in the mitochondrial genomes of insects. Molecular Biology and Evolution 20: 1612–1619. https://doi.org/10.1093/molbev/msg176

Su X, Yang D, Wu X, Sun Y, Qiu JW, Zhang Y (2025) Substantial mitochondrial gene order rearrangements and differential evolution rates within the family Capitellidae (Annelida). Zoosystematics and Evolution 101: 955–967. https://doi.org/10.3897/zse.101.144081

Suyama M, Torrents D, Bork P (2006) PAL2NAL: Robust conversion of protein sequence alignments into the corresponding codon alignments. Nucleic Acids Research 34: W609–W612. https://doi.org/10.1093/nar/gkl315

Tamura K, Stecher G, Kumar S (2021) MEGA11: Molecular Evolutionary Genetics Analysis Version 11. Molecular Biology and Evolution 38: 3022–3027. https://doi.org/10.1093/molbev/msab120

The Galaxy Community (2024) The Galaxy platform for accessible, reproducible, and collaborative data analyses: 2024 update. Nucleic Acids Research 52: W83–W94. https://doi.org/10.1093/nar/gkae410

Thorvaldsdóttir H, Robinson JT, Mesirov JP (2013) Integrative Genomics Viewer (IGV): High-performance genomics data visualization and exploration. Briefings in Bioinformatics 14: 178–192. https://doi.org/10.1093/bib/bbs017

Untergasser A, Nijveen H, Rao X, Bisseling T, Geurts R, Leunissen JA (2007) Primer3Plus, an enhanced web interface to Primer3. Nucleic Acids Research 35: W71–W74. https://doi.org/10.1093/nar/gkm306

Wick RR, Schultz MB, Zobel J, Holt KE (2015) Bandage: Interactive visualization of de novo genome assemblies. Bioinformatics 31: 3350–3352. https://doi.org/10.1093/bioinformatics/btv383

Wong TKF, Ly-Trong N, Ren H, Demotte P, Baños H, Roger AJ, Susko E, Bielow C, De Maio N, Goldman N, Hahn MW, dos Reis M, Vinh LS, Huttley G, Lanfear R, Minh BQ (2026) IQ-TREE 3: Phylogenomic inference software using complex evolutionary models. Molecular Biology and Evolution 43: msag117. https://doi.org/10.1093/molbev/msag117

WoRMS Editorial Board (2026) World Register of Marine Species. https://www.marinespecies.org (Accessed 8 July 2026)

Yu HY, Chu KH, Tsang LM, Ma KY (2024) Incomplete lineage sorting and long-branch attraction confound phylogenomic inference of Pancrustacea. Frontiers in Ecology and Evolution 12: 1243221. https://doi.org/10.3389/fevo.2024.1243221

Supplementary Material 1

File S1

Authors: Matsushima Y, Kano Y, Kakui K (2026)
Data type: .pdf
Explanation notes: The **Table** shows the alignment lengths and optimal substitution models for two rRNA and 13 coding genes (initially partitioned into 41 subsets), Dataset 1. — The **Figure** shows the maximum-likelihood (ML) phylogeny for peracarid crustaceans, based on mitogenome sequences (11,650 characters from 13 protein-coding genes [PCGs] and two rRNA genes; Dataset 1). The dataset was initially partitioned into 41 partitions, representing the three individual codon positions for each of the 13 PCGs and the two separate rRNA genes. These subsets were optimized into a final scheme of 22 partitions. Numbers near nodes are ultrafast bootstrap values (UFBoot). — The Figure shows the assessment of long-branch attraction artifacts using parametric bootstrapping in Dataset 2 (comprising amino acid sequences for 13 PCGs and nucleotide sequences for two rRNAs).

Link: https://doi.org/10.3897/asp.84.e192470.suppl1

Supplementary Material 2

Tables S1–S3

Authors: Matsushima Y, Kano Y, Kakui K (2026)
Data type: .zip
Explanation notes: **Table S1.** Source information for species included in the phylogenetic analyses. — **Table S2.** Alignment lengths and optimal substitution models for the two rRNA and 13 protein-coding genes included in phylogenetic analyses of Dataset 2. In the Length column, amino acid lengths are in bold font. — **Table S3.** Alignment lengths and optimal substitution models for the two rRNA and 13 protein-coding genes included in the phylogenetic analysis of Dataset 3.

Link: https://doi.org/10.3897/asp.84.e192470.suppl2

Supplementary Material 3

Figure S1

Authors: Matsushima Y, Kano Y, Kakui K (2026)
Data type: .tif
Explanation notes: Assessment of long-branch attraction artifacts using parametric bootstrapping in Dataset 2 (comprising amino acid sequences for 13 PCGs and nucleotide sequences for two rRNAs).

Link: https://doi.org/10.3897/asp.84.e192470.suppl3